Dalton Transactions

PAPER

View Article Online
View Journal | View Issue

Cite this: *Dalton Trans.*, 2014, **43**, 15098

Titanium imido complexes stabilised by bis(iminophosphoranyl)methanide ligands: the influence of N-substituents on solution dynamics and reactivity†

Adrien T. Normand,[a] Alexandre Massard,‡[a] Philippe Richard,[a] Coline Canovas,[a] Cédric Balan,[a] Michel Picquet,[a] Audrey Auffrant*[b] and Pierre Le Gendre*[a]

Received 12th March 2014,
Accepted 11th April 2014

DOI: 10.1039/c4dt00746h

www.rsc.org/dalton

Terminal titanium imido complexes of the general formula [Ti(N^{t}Bu)Cl{CH(Ph$_2$PNR)$_2$}] **4** (R = Ph, ^{i}Pr, ^{t}Bu) are reported. These compounds were synthesized from the corresponding Li adducts **3** of BIPMH (bis-(iminophosphoranyl)methanide) and Mountford's complex [Ti(N^{t}Bu)Cl$_2$(Py)$_3$]. The crystal structures of two of the Ti complexes (R = Ph, ^{t}Bu) and two of the Li compounds (R = ^{i}Pr, ^{t}Bu) are reported. Dynamic solution NMR spectroscopy reveals a dynamic isomerisation process in the case of the Ti complex **4c** (R = ^{t}Bu). DFT studies showed that this dynamic process comes from steric repulsion between the imido ligand and the ^{t}Bu N-substituents on the BIPMH ligand. Complexes **4** were tested in alkyne hydroamination; **4a** (R = Ph) displayed modest catalytic activity in the reaction of aniline with phenylacetylene.

Introduction

The coordination chemistry of bis(iminophosphoranyl)methanide and bis(iminophosphoranyl)methanediide ligands (hereafter referred to as BIPMH and BIPM respectively) has been thoroughly studied and reviewed.[1–6] Whilst BIPM complexes are best described as pincer carbene complexes,[4] BIPMHs are analogous to L_2X ligands such as the cyclopentadienyl (Cp) or 1,3-diketiminate (nacnac) ligands.[7,8] However, this analogy is of limited use in order to understand the structure and reactivity of BIPMH complexes. Indeed, negative hyperconjugation plays an important part in BIPMH ligands, which are best described as alternating dipoles with strongly localised charges (Fig. 1), rather than species with a delocalised π-electron system.[9–11]

In contrast to nacnac ligands, for which the observed coordination modes' diversity stems from the presence of both σ- and π-donor fragments,[12,13] most BIPMH complexes display $\kappa^2N,N,\kappa C$ coordination (Fig. 1),[5] as a result of the considerable electron density localised on the methine bridge. However, the extent of the interaction between the carbon atom and the metal centre varies widely, ranging from the covalent bond[14] to almost no interaction at all.[15] A striking illustration of this somewhat unpredictable variability was reported by Stephan in the shape of a chromium-BIPMH dimer for which the crystal structure revealed two isomers with very different Cr–C bond lengths.[16] Thus, BIPMH complexes represent a fascinating class of coordination compounds for the study of the influence of steric, electronic and stereoelectronic factors on the structure and reactivity.

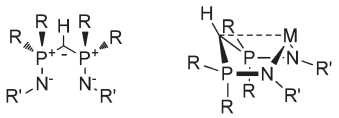

Fig. 1 Alternating dipolar representation of the electronic structure of BIPMH ligands, and boat conformation of their coordination complexes.

Despite the large (and growing) number of BIPMH and BIPM complexes reported to date, titanium complexes of such ligands remain rare. In 1999, Cavell reported the only known example of a Ti-BIPM complex (Fig. 2).[17]

To the best of our knowledge, a Ti-BIPMH complex is yet to be reported,[19] although Hf (**Ia**) and Zr (**Ib**) complexes obtained from the reaction of the corresponding carbene complexes with Brønsted acids are known.[20]

[a]*Institut de Chimie Moléculaire de l'Université de Bourgogne (ICMUB) – UMR CNRS 6302, Université de Bourgogne, UFR Sciences et Techniques, 9 avenue Alain Savary, BP 47870 21078 Dijon, Cedex, France*
[b]*Laboratoire de Chimie Moléculaire, École Polytechnique, UMR CNRS 9168, Route de Saclay, 91128 Palaiseau, Cedex, France. E-mail: audrey.auffrant@polytechnique.edu, pierre.le-gendre@u-bourgogne.fr*

†Electronic supplementary information (ESI) available: CIF files for compounds **3b**, **3c**, **4a**, **4c**; NMR spectra of new compounds and reactivity studies. CCDC 987356–987359. For ESI and crystallographic data in CIF or other electronic format see DOI: 10.1039/c4dt00746h

‡Present address: Laboratoire de Chimie de Coordination, Institut Le Bel, 4 rue Blaise Pascal, CS 90032, 67081 Strasbourg cedex, France.

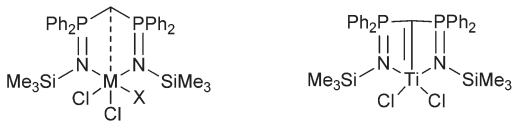

Fig. 2 Relevant group 4 BIPMH and BIPM complexes reported by Cavell.[18]

Additionally, terminal Ti-imido complexes are highly sought-after compounds with interesting reactivity, which stems from the polar nature of the Ti=N bond.[21,22] Most notably, they react with heterocumulenes,[23–25] and are useful pre-catalysts in a variety of reactions, including the important hydroamination of alkynes.[26–29] From a synthetic point of view, the use of the $[Ti(N^tBu)Cl_2(Py)_3]$ precursor developed by Mountford is a versatile method for the preparation of terminal Ti-imido complexes with a variety of ancillary ligands on Ti.[21]

In this paper, we report the synthesis and structural characterization of BIPMH-stabilized Ti-imido complexes, along with preliminary reactivity studies on alkyne hydroamination. We show that the choice of substituents at the BIPMH nitrogen atoms has a profound impact on both the dynamic solution behaviour and the reactivity of these complexes.

Results and discussion

Synthesis and structure

We became interested in the use of BIPMH as stabilizing ligands for Ti-imido species while studying the coordination chemistry of bis(iminophosphorane) ligands (BIP).[30] These are easily obtained from diphosphines following the procedure developed by Le Floch,[10,31] based on the Kirsanov reaction between *in situ* generated bromophosphonium cations and primary amines. With a variety of bis(aminophosphonium) salts **1** in hand, the synthesis of the corresponding BIP **2** by deprotonation with two equivalents of base is straightforward, affording **2a–c** as air-sensitive solids in high yields (Scheme 1). Depending on the substituents on the nitrogens, BIPs can be observed as dipolar (**D**) or alternating dipolar (**A**) forms.[32] Alkyl groups typically favour form **A**, and aromatics give form **D**. This is consistent with the view of a *BIPMH-stabilized* H^+ in

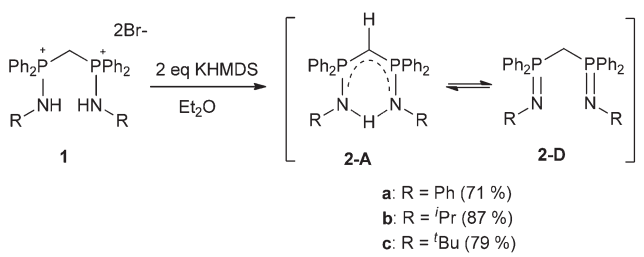

Scheme 1 Synthesis of BIP ligands **2a–c**.

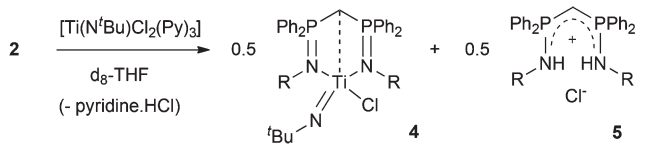

Scheme 2 Formation of BIPMH Ti-imido complexes **4**.

form **A**, which is more favourable with electron-donating groups on the nitrogens. It is noteworthy that the newly synthesized ligand **2c** gives a mixture of both forms (as evidenced by its ^1H and ^{31}P NMR spectra in CD_2Cl_2 and d_8-THF) despite the highly electron-donating nature of the tertiary alkyl groups, whilst **2a** and **2b** are present almost exclusively in **D** and **A** forms, as previously reported.[10]

Reaction of **2** with $[Ti(N^tBu)Cl_2(Py_3)]$ (Scheme 2) invariably afforded BIPMH complexes **4**, together with pyridine hydrochloride and monocation **5**, which was identified notably by the appearance of a new signal in the ^{31}P NMR spectrum (**5a:** 24.3 ppm; **5b:** 31.3 ppm; **5c:** 26.8 ppm). Comparison of the reaction mixtures with independently prepared **4** (*vide infra*) confirmed the concomitant formation of those species. Addition of one equivalent of potassium hexamethyldisilazane (KHMDS) to the reaction mixture enabled clean and complete conversion of the BIP to the Ti imido species for **2a** and **2b** (see ESI, Fig. S4 to S10;† a complex mixture was observed in the case of **2c**). Although the formation of the BIPMH complexes **4** is likely driven by the presence of pyridine in the reaction mixture, it is worth noting that Caulton reported a similar formation of a Ru BIPMH complex in the absence of a base (*i.e.* HCl was released).[14]

Since the formation of BIPMH-stabilised Ti imido complexes **4** appeared to be thermodynamically favoured over that of Ti-BIP species,[33] we turned our attention to their study. We initially envisaged the sequential one-pot reaction of **1** with 3 equivalents of *n*-BuLi and one equivalent of $[Ti(N^tBu)Cl_2(Py)_3]$, however, the material obtained following this procedure appeared to contain considerable amounts of coordinated Br, as evidenced by the isolation of crystals of $[TiBr(BIPMH^{Ph})(\mu\text{-}O)]_2$ after workup.[34] This compound probably results from the hydrolysis of $[Ti(N^tBu)Br(BIPMH^{Ph})]$ and suggest that a Br-free route would be more practical. For this purpose, the use of alkaline metal complexes as BIPMH transfer agents – a strategy already employed by one of us,[31,35,36] and others[3,37–44] – seemed particularly attractive (Scheme 3). Synthesis of lithium compounds **3** was achieved by deprotonation of the corresponding BIP ligands with 1 equiv. of *n*-BuLi. Complexes **3** were obtained as extremely air-sensitive solids; possibly due to their moisture sensitivity, they decomposed over time when the reaction mixtures were left at room temperature for too long (>30 min).

Once in the solid state, they could be stored in a glovebox at −18 °C for months without decomposition. ^1H and ^{31}P NMR spectra were consistent with those reported for similar monomeric structures.[10,15,45–47] Interestingly, only one set of signals was observed for the four P-substituents, suggesting a rapid

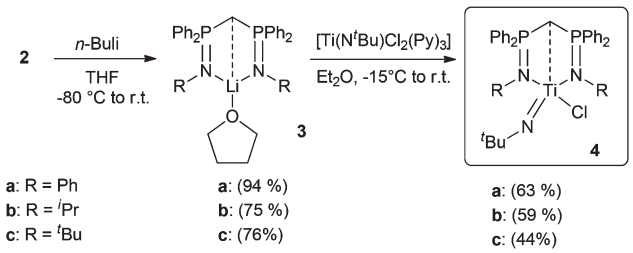

Scheme 3 Synthesis of BIPMH-stabilized Ti-imido complexes by transmetallation with Li compounds.

equilibrium between the two boat conformations. Single crystals suitable for X-ray diffraction were obtained in the case of **3b** and **3c** by slow diffusion of *n*-pentane into a THF solution of each compound at −18 °C. The putative monomeric solution structures were thus confirmed in the solid state (Fig. 3).

It is worth mentioning that despite their synthetic utility, there are only a limited number of structurally characterized group 1 BIPMH complexes,[10,15,45–49] of which only 5 have monomeric Li structures (Fig. 4). The most salient feature of these solid-state structures is the high variability of the Li–C^1 bond distance between the metal and the methine bridge, ranging from 2.545 (**3c**) to 3.196 Å (**3g**).

These distances are well above the sum of covalent radii for Li and sp^2-C (2.01 ± 0.09 Å),[50] and considerably shorter than the sum of van der Waals radii (3.89 Å), a common structural

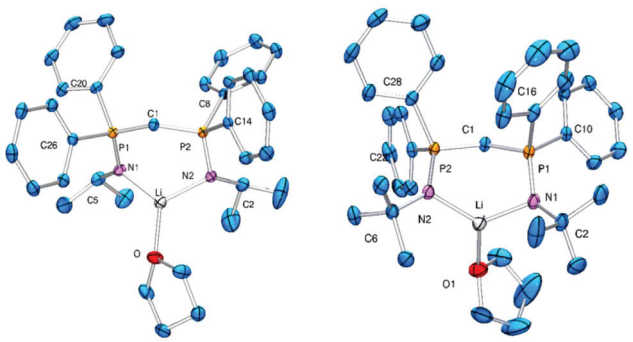

Fig. 3 POV-RAY depiction of **3b** and **3c** (thermal ellipsoids drawn at the 50% probability level).

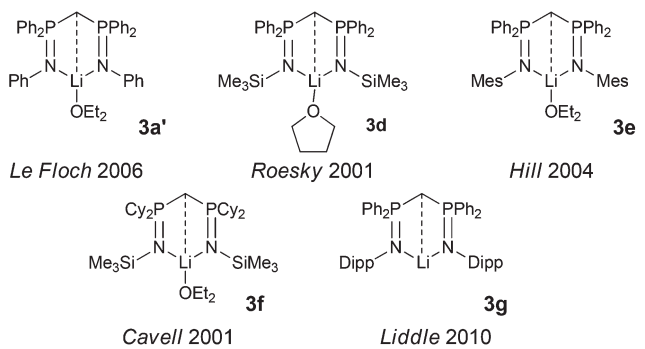

Fig. 4 Structurally characterised monomeric Li compounds.[10,15,45–47]

feature of BIPMH complexes.[5] Table 1 gives selected bond distances and angles for **3b–c** and relevant literature compounds.

For BIPMH ligands with aryl substituents at the nitrogens, increasing steric bulk results in an opening of the 6-membered metallacycle along the Li–C^1 axis, whilst in the case of alkyl substituents (*e.g.* **3b** and **3c**), the opposite trend is observed. As a result of the poorer interaction between Li and C^1 in "open boat" structures, the interaction between Li and N becomes stronger and Li–N bond distances are shortened (compare **3b** and **3c**). Other notable features are (*i*) the trigonal planar geometry around N (sum of angles close to 360°) and (*ii*) the sp^2 hybridization of C^1 suggested by P^1–C^1–P^2 angles of 125.9 (**3a′**) to 134.6° (**3e**). Again, these features are commonplace for BIPMH complexes, and they are also observed in Ti complexes **4** (*vide infra*). Reaction of Li compounds **3** with [Ti(N^{t}Bu)Cl_2(Py)$_3$] afforded complexes **4** in moderate to good yield (Scheme 3). The presence of the terminal Ti-imido group is suggested by the IR spectra of **4**, with medium bands in the 1200–1260 cm^{-1} region and strong bands in the 520–550 cm^{-1} region, as reported by Mountford.[51]

Upon coordination to Ti, the four phenyl substituents on the phosphorus atoms give rise to two sets of signals in the ^{1}H NMR spectra, consistent with the now diastereotopic relationship of those groups. In the case of **4b**, the CH_3 groups of the ^{i}Pr substituent are also diastereotopic and resonate as two doublets at 1.77 and 0.91 ppm ($^3J_{HH}$ = 7.2 Hz). Complexes **4a** and **4c** gave crystals suitable for X-ray diffraction by slow diffusion of *n*-pentane into CH_2Cl_2 solutions of the complexes at −18 °C (Fig. 5).[52] Relevant structural parameters are given in Table 2, together with those of **Ia** and **IIa** (Fig. 2) for comparison.

The metallacycles in both complexes exhibit the same boat conformation with the Cl ligand located in the axial position. At 2.599(2) (**4a**) and 2.557(2) Å (**4c**), the Ti–C^1 distances are longer than the sum of covalent radii for Ti and sp^2 C (2.33(8) Å),[50] and considerably smaller than the sum of van der Waals radii (4.23 Å).[53]

This contrasts with BIPMH-Hf complex **Ia**, which features an elongated covalent Hf–C^1 bond (2.438(6) *vs.* 2.48(10) Å). As expected, the Ti–C^1 distance in BIPM complex **IIa** (2.008(4) Å) is much shorter than in **4a** and **4c**. One notable variation when comparing **4a** and **4c** with their Li analogues **3a** and **3c** is the somewhat shorter P–N bond distances in the latter (−0.03 Å for Ph and −0.04 Å for ^{t}Bu). This difference could originate from higher ligand-to-metal charge transfer in Ti complexes, hence decreased charges on the nitrogens and a weaker interaction between N and P.[11] Steric factors also seem to play an important part in the differences between Ti complexes and Li adducts. For instance, one could expect the presence of the ^{t}Bu imido group in Ti complexes to impact the geometry of the BIPMH ligand itself. Consistent with this view, P–N–C angles are narrower in **4a** and **4c** compared to **3a′** and **3c**, and the effect is more pronounced for **4c** than **4a** (−4.7 *vs.* −1.2°), in line with the considerably more bulky nature of ^{t}Bu compared to Ph. Further comparison between both complexes shows that the presence of the ^{t}Bu group causes a small but noticeable

Table 1 Selected bond distances (Å) and angles (°) for monomeric Li adducts of BIPMH

	3b	3c	3a′[10]	3e[47]	3g[15]
d_{Li-C}[1]	2.736(4)	2.545(3)	2.578(4)	2.999(5)	3.196(9)
d_{Li-Nj}	1.954(4)	1.980(4)	1.961(3)	1.952(5)	1.882(8)
	1.939(4)	1.977(3)	1.989(3)	1.979(4)	1.880(7)
$d_{P/N}$	1.5868(16)	1.585(2)	1.603(1)	1.597(2)	1.600(4)
	1.5899(16)	1.585(2)	1.597(1)	1.585(2)	1.607(4)
d_{C^1-P}	1.7191(19)	1.730(2)	1.720(3)	1.725(2)	1.700(4)
	1.726(2)	1.723(2)	1.722(2)	1.713(2)	1.698(5)
d_{Li-O}	1.917(4)	1.954(3)	1.954(3)	1.965(5)	—
P–C[1]–P	131.25(10)	130.00(9)	125.9(1)	134.58(16)	134.7(3)
N–Li–N	116.51(19)	119.7(2)	116.14(14)	114.9(2)	117.7(4)
P–N–E[a]	126.41(14)	129.98(12)	126.18(10)	126.59(18)	127.2(3)
	123.65(14)	133.19(11)	128.93(11)	130.68(17)	122.5(3)
$\sum\alpha$(N)	359.8(5)	355.6(4)	357.0(4)	359.2(5)	359.3(9)
	353.7(5)	358.9(4)	359.8(4)	358.2(5)	358 (1)

[a] E = C, Si.

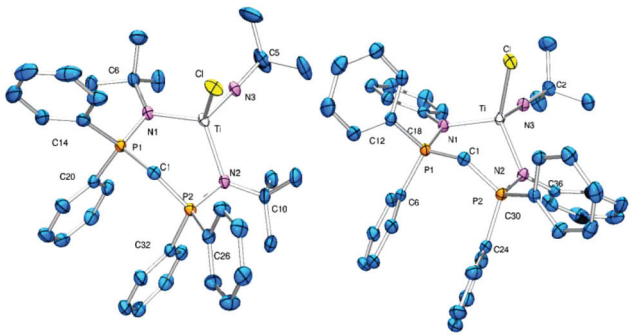

Fig. 5 POV-RAY depiction of **4a** and **4c** (thermal ellipsoids drawn at the 50% probability level).

Table 2 Selected bond distances (Å) and angles (°) for **4a**, **4c** and relevant compounds from the literature

	Ia	IIa	4a	4c
d_{M-C}[1]	2.438(6)	2.008(4)	2.599(2)	2.557(2)
d_{M-N}	2.258(5)	2.061(4)	2.052(2)	2.070(2)
	2.240(5)	2.089(4)	2.040(2)	2.071(2)
$d_{P/N}$	1.614(5)	1.621(4)	1.636(2)	1.626(2)
	1.616(5)	1.622(4)	1.630(2)	1.625(2)
d_{C^1-P}	1.760(7)	1.678(5)	1.726(2)	1.726(2)
	1.759(7)	1.679(5)	1.729(2)	1.727(2)
d_{Ti-Cl}	—	2.2761(16)	2.3559(6)	2.3741(5)
		2.2827(15)		
d_{Ti-N}[3]	—	—	1.670(2)	1.715(2)
P–C[1]–P	122.0(3)	157.4(3)	127.1(1)	128.2(1)
N–M–N	95.56(17)	148.92(14)	108.53(7)	112.13(6)
Ti–N[3]–C	—	—	165.4(2)	168.2(1)
Cl–Ti–N[3]	—	—	101.62(6)	99.00(5)
P–N–E[a]	130.8(3)	134.1(2)	125.93(14)	126.50(13)
	132.7(3)	132.3(2)	126.71(14)	126.84(12)
$\sum\alpha$(N)	359.8(8)	359.5(6)	359.9(4)	358.1(3)
	357.6(8)	359.5(8)	359.2(4)	357.8(3)

[a] E = C, Si.

distortion of the boat metallacycle, principally by widening the N–Ti–N angle (+3.60°). Finally, a combination of steric and electronic factors can be invoked to explain the shorter Ti-imido bond distance in **4a** (1.670(2) Å) compared to **4c** (1.715(2) Å): indeed, the steric repulsion between ^{t}Bu groups, as well as the greater electron density of the [TiCl(BIPMH$^{t\mathrm{Bu}}$)] fragment (due to the more electron-donating ^{t}Bu compared to Ph), both mitigate against a short Ti-imido bond.

In light of the rather similar solid-state structures of **4a** and **4c**, it might seem surprising that, unlike **4a** and **4b**, **4c** would exist as a mixture of two isomers in solution. Indeed, we invariably observed a small amount (~10%) of additional product by NMR for the latter. By ^{31}P NMR spectroscopy, a signal at 15.6 ppm was observed, and several additional signals are also present in the ^{1}H NMR spectrum, most notably a triplet at 2.49 ppm ($^2J_{PH}$ = 3.8 Hz) ascribed to a bridging methine group, and ^{t}Bu signals at 1.30 and 1.24 ppm; ^{13}C NMR spectroscopy also reveals a pattern of signals paralleling that of the main product. Crucially, an EXSY NMR experiment revealed that both species are involved in a chemical exchange (Fig. 6).

Altogether, these observations suggest a rapid dynamic equilibrium between two boat forms **4c-ax** and **4c-eq**, (Scheme 4; in the following discussion, both isomers will be distinguished by the axial or equatorial position of the Cl ligand).[55]

Variable temperature NMR spectroscopy experiments enabled us to determine the values of the equilibrium

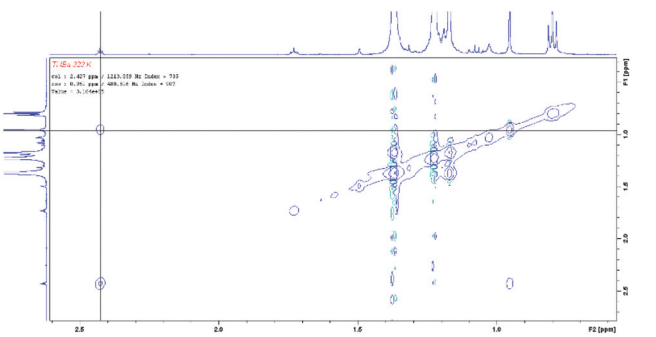

Fig. 6 EXSY NMR, high field region (500 MHz, CD_2Cl_2, 323 K, 300 ms mixing time).[54] Black lines indicate the exchanging signals.

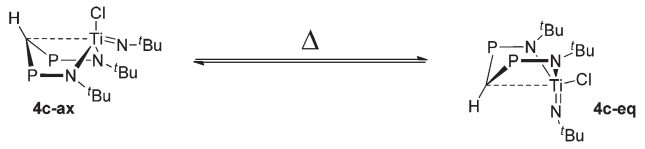

Scheme 4 Dynamic equilibrium between the two boat isomers of **4c**.

constant at different temperatures in the 273–333 K range by integration of the CH bridge signal intensity in **4c-ax** and **4c-eq**. Using the relationship $\ln K = -\Delta G^\circ/RT$, values of ΔH° = 12.6 ± 1.4 kJ mol^{-1} and ΔS° = 24.9 ± 4.7 J mol^{-1} K^{-1} were obtained (see ESI, Fig. S3†).

Computational studies

The isomerisation equilibrium described above is not surprising in itself. Such dynamic solution behaviour has been reported in the case of related bimetallic phosphinoamide Ti/Pt complexes with a PtX_2 bridge isolobal to CH.[56] Also, as mentioned above, two structural isomers of the complex $[Cr(\mu\text{-}Cl)(HC(PPh_2NSiMe_3)_2)]_2$ with different Cr–C bond lengths (2.26 *vs.* 2.92 Å) were previously reported by Stephan.[16] More intriguing is the fact that **4a** and **4b** do not display a similar behavior.[57] One possible explanation could be the increased steric repulsion between the three ^{t}Bu groups in the axial Cl isomer (**4c-ax**), which would reduce the energy gap between both isomers and make the energy level of the equatorial Cl isomer (**4c-eq**) accessible at room temperature. To test this hypothesis, we conducted DFT calculations at the B3LYP level of theory (see the Computational details section) on **4b** and **4c**, as well as on **4d** (the NMe imido analogue of **4c**).

Calculated energies for the different isomers of the ^{t}Bu and ^{i}Pr complexes are in agreement with the fact that the axial-Cl isomer is the experimentally preferred one. For **4c**, the free energy difference between both isomers is calculated to be 5.1 kJ mol^{-1} at 298.15 K, which corresponds to a **4c-eq**/**4c-ax** ratio of 0.128 (for an experimental value of 0.124(5)). For **4b**, comparison between theory and experiment is more difficult since the axial isomer was the only observed species, however, it is possible to assign an upper limit (0.01) to the equilibrium constant, and thus a lower limit (11 kJ mol^{-1}) to ΔG°. The latter is consistent with the calculated value of 22.1 kJ mol^{-1}. Replacing the ^{t}Bu group of the imido ligand in complex **4c** by a methyl group leads to a higher energy gap between both isomers in complex **4d** (18.5 kJ mol^{-1}) consistent with the hypothesis that steric repulsion between the N-substituents of the BIPMH and the imido ligands destabilizes the axial isomer of **4c**, thus facilitating the isomerisation.

It is quite remarkable that such a seemingly small change of N-substituents should trigger observable isomerisation equilibrium, and this phenomenon highlights the subtle steric interactions at play in BIPMH complexes. Therefore, it is of interest to compare the experimental (**4c-ax**) and calculated (**4c-ax/eq**, **4b-ax/eq**, **4d-ax/eq**) structures, see Table 3.

As is usually the case with DFT methods in general, and the B3LYP functional in particular, the calculated gas-phase geometry of **4c-ax** is close to the experimental solid-state structure. The highest relative error (+4%) is the Ti–C^1 distance, which corresponds to an absolute error of 0.108 Å. This discrepancy is likely due to crystal packing effects which are more important for bonds with a large electrostatic contribution.[58] Other bond distances typically fall within 0.03 Å of the experimental values (3° for angles). In the case of **4b**, the low quality of the obtained crystals precludes a detailed comparison of structural parameters, however, it is worth noting that the orientation of the ^{i}Pr substituents was similar in both cases, with CH_3 groups pointing towards the metal, as observed for the Li adduct **3b**.

Comparing the calculated gas-phase structures of the axial and equatorial isomers, it appears that the most important difference resides in the global shape of the metallacycles. For axial isomers, the boat has a relatively open structure, with Ti–C^1 distances ranging from 2.592 Å (**4d-eq**) to 2.753 Å (**4b-eq**). The less favorable equatorial isomers have considerably shorter (−0.21 to −0.296 Å) Ti–C^1 distances, thereby increasing ring strain considerably (see Fig. 7 for **4c**). In the

Table 3 Comparison of bond distances (Å) and angles (°) for **4c** and calculated isomers of **4b**, **4c**, and **4d**

	4c[a]	**4c-ax**[b]	**4c-eq**[b]	**4b-ax**[b]	**4b-eq**[b]	**4d-ax**[b]	**4d-eq**[b]
d_{Ti-C^1}	2.557(2)	2.665	2.377	2.753	2.457	2.592	2.382
d_{Ti-Nj}	2.070(2)	2.103	2.169	2.072	2.138	2.086	2.156
	2.071(2)	2.106	2.157	2.072	2.145	2.090	2.161
$d_{P/N}$	1.626(2)	1.650	1.631	1.652	1.632	1.648	1.631
	1.625(2)	1.651	1.632	1.652	1.632	1.649	1.631
d_{C^1-P}	1.726(2)	1.736	1.760	1.733	1.753	1.744	1.759
	1.727(2)	1.736	1.761	1.733	1.749	1.744	1.758
d_{Ti-Cl}	2.3741(5)	2.361	2.371	2.359	2.350	2.368	2.368
d_{Ti-N^3}	1.715(2)	1.706	1.702	1.700	1.702	1.698	1.699
P–C^1–P	128.2(1)	131.59	133.24	127.97	131.71	130.06	134.02
N–Ti–N	112.13(6)	115.45	115.86	108.41	114.12	111.47	115.84
Ti–N^3–C	168.2(1)	167.10	165.82	163.35	166.74	174.20	169.55
Cl–Ti–N^3	99.00(5)	101.59	101.55	102.45	102.34	103.12	102.22
P–N–C	126.50(13)	126.18	128.91	120.35	122.07	128.72	128.71
	126.84(12)	126.05	128.52	120.29	121.69	128.75	128.50

[a] Experimental structure. [b] Gas phase theoretical structures.

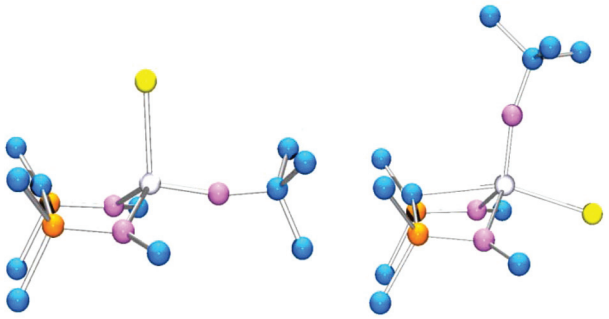

Fig. 7 Calculated structures for **4c-ax** (left) and **4c-eq** (right). Ph and ^{t}Bu groups on the BIPMH ligand removed for clarity.

case of **4c-eq** and **4d-eq**, the Ti–C^{1} distances are now within the sum of covalent radii (2.33(8) Å).[50]

The reason for the longer Ti–C^{1} bond distance in the axial isomers is somewhat unclear, as this seems to push the imido ^{t}Bu group closer to the BIPMH N-substituents. The same can be said about the shorter Ti–C^{1} bond distance in the equatorial isomers, for which there is *a priori* no obvious reason. One possible explanation could be the greater *trans* influence of the imido ligand compared to the chloride.[59] Nevertheless, the shapes of the experimental and computational structures are counter-intuitive, and probably result from a subtle interplay of steric and electronic factors.

Whilst our calculations do not point to an obvious reason for the preference of the axial isomer over the equatorial one, they do reveal differences between **4b-ax** and **4c-ax**; these parallel the experimentally observed trends between **4a** and **4c** in their crystal structures, and support the hypothesis of a sterically induced destabilisation of the major isomer of **4c**. Indeed, upon replacing ^{i}Pr with ^{t}Bu, we observe the opening of the P–C^{1}–P (+3.62°), N–Ti–N (7.04°) and P–N–C angles (+5.8° on average). The shape of the metallacycle also changes, with a widening of the φ1 (NTiN/PPNN) dihedral angle (+4.72°), and a narrowing of the φ2 (PC^{1}P/PPNN) dihedral angle (−5.93°). By contrast, these differences are much less pronounced between the equatorial isomers (**4b-eq** *vs.* **4c-eq**), except for the P–N–C angles which remains wider in **4c-eq** (+6.8° on average). These data indicate that the presence of ^{t}Bu N-substituents exerts a considerable influence by pushing the P and N substituents of the BIPMH away from each other.[60] This brings the ^{t}Bu groups closer to the imido ligand in the axial isomer, thus distorting the boat metallacycle and reducing the energy gap between both isomers; ultimately, the inversion of the boat is facilitated. Therefore, regardless of the exact reasons for the preference of the axial isomer over the equatorial one, our calculations clearly show that steric factors are decisive to explain the different behavior of **4b** and **4c**, as observed experimentally.

Reactivity and catalysis

In comparison to the number of reports focusing on their coordination chemistry, catalytic applications of BIPMH complexes are rare. Most reports focus on lanthanides,[35,36,38–41,61–66] although other metals have been investigated, notably Ca and Mg (ring-opening polymerisation),[7] Al (ethylene polymerisation),[67] Cr (ethylene oligomerization),[31] Zn (ring-opening polymerisation),[68] Y (intramolecular hydroamination of unsaturated substrates),[38,40] and Zr (ethylene polymerisation).[8] Given the widespread use of terminal Ti imido complexes in alkyne hydroamination,[26–29] it was interesting to evaluate the potential of complexes **4** in this reaction. The results are presented in Table 4. Overall, the catalytic activity of these complexes was disappointing, and in the case of **4b**, nonexistent (entry 1). Indeed, aniline and phenylacetylene are rather forgiving substrates, and only in the case of **4a** was it possible to obtain appreciable yields of hydroamination products (entry 3), albeit under forcing conditions and with low selectivity. In light of the mechanistic studies by Bergman,[69] and Doye,[70] and considering the structure of complexes **4** compared to active hydroamination catalysts such as [CpTi(N^{t}Bu)Cl(Py)] or [CpTi(NAr)(NHAr)], it appears that a free coordination site is necessary in order to initiate the catalytic cycle.

Table 4 Catalytic hydroamination with **4**

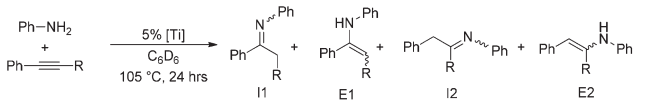

Entry	Alkyne	Catalyst	Conv.[a,b] (%)	Yield **I1**[b] (%)	Yield **E2**[b] (%)
1	PhCCH	**4b**	10	0	0
2	PhCCH	**4c**	24	Traces	7
3	PhCCH	**4a**	84	19	13
4	PhCCPh	**4a**	5	Traces	0

Reagents and conditions: alkyne and aniline (0.5 mmol), catalyst (0.025 mmol), 0.102 M solution of 1,3,5-trimethoxybenzene in C_6D_6 (1 mL), 24 h, 105 °C. [a] Based on remaining aniline. [b] Calculated by ^{1}H NMR, based on the average of two runs.

This does not seem to be the case with **4**, which means that these complexes must find an energetically costly way to accommodate an incoming alkyne molecule, be it Cl dissociation, BIPMH boat-chair isomerisation or (possibly in the case of **4a**) an increase in the coordination number. Thus, further development of BIPMH Ti imido complexes should focus on solutions aimed at creating a free coordination site on Ti, *e.g.* by replacing Cl by a more labile ligand.

Although the results presented above are only preliminary,[71] and show that at the very least, precatalyst design needs to be improved, they indicate that aryl substituents on the BIPMH nitrogen atoms are more likely to give active catalysts. There could be two reasons for this: firstly, aryl groups are less electron-donating and will give rise to more Lewis acidic complexes, a feature which is expected to increase the reactivity of coordinated alkynes; secondly, the increased activity of **4a** could also result from the greater steric flexibility of the Ph substituent (compared to ^{i}Pr or ^{t}Bu) which is able to

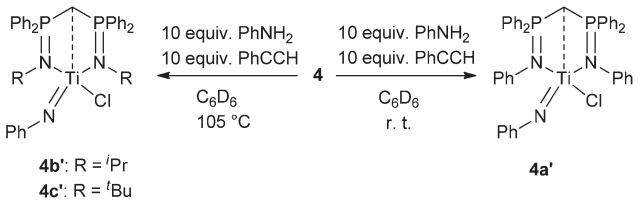

Scheme 5 *In situ* formation of Ti=NPh species.

relieve steric strain around Ti by rotation around the N–C bond. As an illustration of the greater reactivity of **4a**, we followed the fate of complexes **4** in the presence of 10 eq. of aniline and phenylacetylene by ^{1}H and ^{31}P NMR spectroscopy. Whilst **4a** showed complete imido group exchange at room temperature,[51] **4b** and **4c** had to be heated to 105 °C for several hours for the exchange to proceed (Scheme 5). Remarkably, after heating for 13 h at this temperature, virtually no other P-containing products were observed (^{31}P NMR: δ = 21.6 (**4a′**), 26.7 (**4b′**), 22.9 (**4c′**) ppm); additionally, **4a′** and **4c′** (to a lesser extent) showed hydroamination activity (significant amounts of I1 and E2 were observed, see ESI Fig. S11 to S22†). These observations are consistent with the increased catalytic activity of **4a** compared to **4b** and **4c**, which is likely to originate from a combination of steric and electronic factors.

Finally, given the robustness of these complexes even under forcing conditions, it was interesting to probe their reactivity towards water. Indeed, one of the caveats of using oxophilic group 4 metals for hydroamination is that reaction substrates (particularly the amine partner) need to be thoroughly dried for the reaction to proceed. Clearly, this sensitivity impedes industrial applications of such catalysts.

Interestingly, upon reaction with increasing amounts of water or ^{i}PrOH, **4b** and **4c** showed a rather peculiar behaviour. Indeed, only the starting complexes and monocations **5** were observed. After addition of 2 equivalents of water (or 4 equivalents of ^{i}PrOH), the only products observed by ^{1}H and ^{31}P NMR spectroscopy were ^{t}BuNH$_2$ and **5** (and [Ti(O^{i}Pr)$_4$] in the case of ^{i}PrOH). In the case of **4a**, intermediate products were observed by ^{31}P NMR spectroscopy (including **2a**), but the global outcome of the reaction was the same as that observed with **4b** and **4c** (Scheme 6), the only notable difference being the presence of small amounts of **2a**, probably due to its lower basicity compared to **2b** and **2c** (see ESI, Fig. S23 to S30†). Overall, these results highlight the high basicity of the BIPMH ligand in **4**, and show that depending on the N-substituents, the Achilles' heel of these complexes in terms of moisture sensitivity might not be the imido ligand, but the BIPMH.

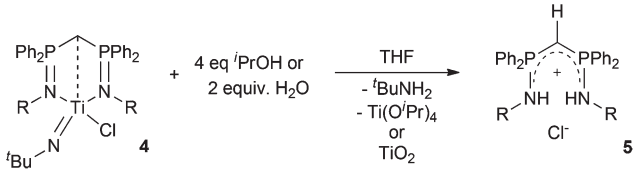

Scheme 6 Hydrolysis/alcoholysis of **4**.

Conclusion

We have reported the first examples of Ti imido complexes stabilized by a BIPMH ligand, in addition to new Li adducts of BIPMH. Their structure has been studied both experimentally (X-ray, dynamic solution NMR spectroscopy) and theoretically (DFT). We have shown that these compounds are very sensitive to steric effects, since changing the N-substituents of the BIPMH from ^{i}Pr to ^{t}Bu brings about a dynamic equilibrium between two isomers of the metallacycle. Finally, we tested complexes **4** in alkyne hydroamination; whilst phenyl substituted complex **4a** showed modest catalytic activity, alkyl substituted complexes **4b** and **4c** were almost completely inactive. This contrasting behavior was mirrored by the rate of imido group exchange in the presence of aniline, with **4a** being much more reactive. The globally unsuitable nature of BIPMH as a supporting ligand for Ti in hydroamination could be due to its strong electron-donating nature, or to coordinative saturation at Ti. In any case, improved catalytic activity could be achieved by freeing a coordination site on Ti, or adding electron-withdrawing substituents on the BIPMH ligand.

Computational details

The theoretical calculations were performed by using Jaguar v. 5.5[72] using the DFT B3LYP method with a 6-31G** basis for most atoms, 6-311+G** for C[1] and LACV3P+** for the titanium atom. The frequencies were checked at the end of the geometry minimizations. The calculations were performed by using HPC resources from DSI-CCUB (Université de Bourgogne).

Experimental

General conditions

All reactions were carried out under Ar using conventional Schlenk techniques or in a N_2 glovebox. Toluene, CH_2Cl_2, Et_2O, pentane and THF were dried using an MBRAUN SPS 800 solvent purification system or distilled under Ar from appropriate drying agents and either used directly or stored under N_2 in the glovebox. Deuterated solvents were dried by passage through a short column of activated neutral alumina (Brockman grade II) and stored over activated 3 Å molecular sieves in the glovebox, either at room temperature (C_6D_6) or at −18 °C (d_8-THF, CD_2Cl_2). Alumina and molecular sieves were activated by overnight heating above 230 °C *in vacuo*. Salts **1a–c** were synthesized according to literature procedures,[10,31] except hygroscopic **1b** which had to be dried by successive azeotropic distillation with toluene. Compounds **2a–b** and **3a–b** were previously reported but were incompletely characterized, or NMR data were reported in different solvents.[10,31,73,74] All other reagents were commercially available and used as received.

All of the analyses were performed at the "Plateforme d'Analyse Chimique et de Synthèse Moléculaire de l'Université de Bourgogne", or at the elemental analysis service of London

Metropolitan University. The identity and purity of the compounds were unambiguously established using elemental analysis, high-resolution mass spectrometry, X-ray diffraction, NMR and IR spectroscopy. High resolution mass spectra were recorded on a Thermo LTQ Orbitrap XL ESI-MS spectrometer. NMR spectra (^{1}H, ^{31}P, ^{13}C) were recorded on Bruker 300 Avance III, 500 Avance III, or 600 Avance II spectrometers. Chemical shifts are quoted in parts per million (δ) relative to TMS (for ^{1}H and ^{13}C) or 85% H_3PO_4 (for ^{31}P). For ^{1}H and ^{13}C spectra, values were determined by using solvent residual signals (*e.g.* $CDHCl_2$ in CD_2Cl_2) as internal standards. In the case of ^{31}P NMR, a capillary filled with 85% H_3PO_4 was placed in the NMR tube for the characterization of new compounds. IR spectra were recorded on a Bruker Vertex 70v FTIR spectrophotometer fitted with a Globar MIR source, a Ge/KBr (MIR) or silicium (FIR) beam splitter, a DLaTGS detector and a diamond ATR module.

Preparations

Preparation of ligand 2a. Salt **1a** (5.360 g, 6.880 mmol) was suspended in Et_2O (40 mL) at room temperature, and a suspension of KHMDS (2.750 g, 13.76 mmol) in Et_2O (30 mL) was cannulated onto the suspension. The resulting pale yellow mixture was stirred for 4 h and filtered over Celite®. The filtered solid was rinsed with Et_2O. The clear yellow solution thus obtained was evaporated and extensively dried *in vacuo* to remove hexamethyldisilazane. Compound **2a** was isolated in 71% yield (2.78 g). The purity of the material thus obtained (assessed by ^{1}H and ^{31}P NMR spectroscopy) was sufficient for further reaction. An analytically pure sample suitable for elemental analysis was obtained by recrystallization from a THF–*n*-pentane mixture.

Elemental analysis: calcd for $C_{37}H_{32}N_2P_2$: C, 78.43; H, 5.69; N, 4.94. Found: C, 78.34; H, 5.84; N, 5.03. HRMS (ESI-pos): calcd for $C_{37}H_{33}N_2P_2$ $[M + H]^+$: 567.21135. Found: 567.20870 (−4.7 ppm). FTIR (ATR): 1589 (m), 1490 (m), 1480 (m), 1328 (br, s), 1308 (m), 1103 (br, m), 1047 (m), 770 (br, m), 754 (m), 717 (m), 704 (m), 688 (s), 486 (s), 401 (m) cm^{-1}. ^{1}H NMR (500 MHz, CD_2Cl_2, 300 K): δ = 7.70 (m, 8H, *o*-Ph_2P), 7.44 (app t, $^{3}J_{HH}$ = 7.5 Hz, 4H, *p*-Ph_2P), 7.33 (m, 8H, *m*-Ph_2P), 6.92 (app t, $^{3}J_{HH}$ = 7.9 Hz, 4H, *m*-PhN), 6.58 (tt, $^{3}J_{HH}$ = 7.3 Hz, $^{4}J_{HH}$ = 1.0 Hz, 2H, *p*-PhN), 6.49 (app d, $^{3}J_{HH}$ = 7.7 Hz, 4H, *o*-PhN), 3.72 (app t, $^{2}J_{PH}$ = 13.6 Hz, 2H, PCH_2P). ^{13}C{^{1}H} NMR (126 MHz, CD_2Cl_2, 300 K): δ = 151.2 (s, i-PhN), 132.4 (app t, $^{2}J_{PC}$ = 4.9 Hz, *o*-Ph_2P), 131.9 (s, *p*-Ph_2P), 131.1 (d, $^{1}J_{PC}$ = 98.2 Hz, i-Ph_2P), 129.0 (s, *m*-PhN), 128.8 (app t, $^{2}J_{PC}$ = 6.1 Hz, *m*-Ph_2P), 123.3 (m, *o*-PhN), 117.5 (s, *p*-PhN), 30.5 (t, $^{1}J_{PC}$ = 63.6 Hz, PCH_2P). ^{31}P{^{1}H} NMR (202 MHz, CD_2Cl_2, 300 K): δ = −0.9 ($\nu_{1/2}$ = 9 Hz).

Preparation of ligand 2b. Salt **1b** (4.95 g, 7.50 mmol) was suspended in Et_2O (40 mL) at 0 °C, and a solution of KHMDS (2.750 g, 15.0 mmol) in Et_2O (30 mL) at room temperature was cannulated onto the suspension. The resulting pale yellow mixture was stirred for 3 h and filtered over Celite®. The filtered solid was rinsed with Et_2O. The clear yellow solution thus obtained was evaporated and extensively dried *in vacuo* to remove hexamethyldisilazane. Compound **2b** was isolated in 87% yield (3.25 g). The purity of the material thus obtained (assessed by ^{1}H and ^{31}P NMR spectroscopy) was sufficient for further reaction. An analytically pure sample suitable for elemental analysis was obtained by recrystallization from a THF–*n*-pentane mixture.

Elemental analysis: calcd for $C_{31}H_{36}N_2P_2$: C, 74.68; H, 7.28; N, 5.62. Found: C, 74.56; H, 7.39; N, 5.63. HRMS (ESI-pos): calcd for $C_{31}H_{37}N_2P_2$ $[M + H]^+$: 499.24265. Found: 499.24115 (−3.0 ppm). FTIR (ATR): 2961 (w), 1432 (m), 1213 (m), 1192 (m), 1176 (m), 1100 (m), 978 (m), 745 (m), 736 (m), 694 (s), 554 (m), 527 (m), 502 (br, s) cm^{-1}. ^{1}H NMR (500 MHz, d_8-THF, 300 K): δ = 7.70 (m, 8H, *o*-Ph_2P), 7.39–7.27 (m, 12H, *p*- and *m*-Ph_2P), 7.04 (br s, 1H, N*H*), 3.42 (t, $^{2}J_{PH}$ = 13.2 Hz, PCH_2P of minor D form), 3.24 (d of heptuplet, $^{3}J_{PH}$ = 16.8 Hz, $^{3}J_{HH}$ = 6.2 Hz, 2H, C*H*$(CH_3)_2$), 0.96 (d, $^{3}J_{HH}$ = 6.2 Hz, 12H, CH(CH_3)$_2$), 0.81 (t, $^{2}J_{PH}$ = 4.1 Hz, 1H, PC*H*P). ^{13}C{^{1}H} NMR (126 MHz, d_8-THF, 300 K): δ = 138.6 (d, $^{1}J_{PC}$ = 95.4 Hz, i-Ph_2P), 132.4 (app t, $^{2}J_{PC}$ = 4.9 Hz, *o*-Ph_2P), 130.3 (s, *p*-Ph_2P), 128.2 (app t, $^{2}J_{PC}$ = 5.7 Hz, *m*-Ph_2P), 45.5 (s, *C*H$(CH_3)_2$), 27.5 (m, two overlapping CH(*C*H_3)$_2$), 9.5 (t, $^{1}J_{PC}$ = 134.5 Hz, P*C*HP). ^{31}P{^{1}H} NMR (202 MHz, d_8-THF, 300 K): δ = 26.2 (major A form, $\nu_{1/2}$ = 3 Hz), −4.2 (minor D form, $\nu_{1/2}$ = 5 Hz).

Preparation of ligand 2c. Salt **1c** (5.16 g, 7.50 mmol) was suspended in Et_2O (40 mL) at 0 °C, and a solution of KHMDS (2.99 g, 15.0 mmol) in Et_2O (30 mL) at room temperature was cannulated onto the suspension. The resulting pale yellow mixture was stirred for 3 h and filtered over Celite®. The filtered solid was rinsed with Et_2O. The clear yellow solution thus obtained was evaporated and extensively dried *in vacuo* to remove hexamethyldisilazane. Compound **2c** was isolated as a mixture of alternating dipolar (**2c-A**, minor) and dipolar (**2c-D**, major) forms in 79% yield (3.11 g). The purity of the material thus obtained (assessed by ^{1}H and ^{31}P NMR spectroscopy) was sufficient for further reaction. An analytically pure sample suitable for elemental analysis was obtained by recrystallization from a THF–*n*-pentane mixture.

Elemental analysis: calcd for $C_{33}H_{40}N_2P_2$: C, 75.26; H, 7.66; N, 5.32. Found: C, 75.19; H, 7.75; N, 5.37. HRMS (ESI-pos): calcd for $C_{33}H_{41}N_2P_2$ $[M + H]^+$: 527.27395. Found: 527.27421 (0.5 ppm). FTIR (ATR): 2962 (m), 1433 (m), 1272 (br, s), 1216 (m), 1106 (m), 1094 (m), 803 (m), 738 (s), 719 (m), 704 (m), 697 (s), 534 (m), 502 (m), 460 (m), 445 (m), 376 (m), 366 (m), 154 (br, m) cm^{-1}. ^{1}H NMR (500 MHz, CD_2Cl_2, 300 K): δ = 7.76 (m, 8H, *o*-Ph_2P of **2c-A**), 7.67 (m, 8H, *o*-Ph_2P of **2c-D**), 7.41–7.30 (m, *p*- and *m*-Ph_2P of both forms), 7.26 (m, *p*- and *m*-Ph_2P of both forms), 6.13 (br s, 1H, N*H* of **2c-A**), 3.35 (t, $^{2}J_{PH}$ = 13.6 Hz, PCH_2P of **2c-D**), 1.08 (s, 9H, ^{t}Bu of **2c-D**), 1.06 (s, 9H, ^{t}Bu of **2c-A**), n.o. (PC*H*P of **2c-A**). ^{13}C{^{1}H} NMR (126 MHz, CD_2Cl_2, 300 K): δ = 139.3 (d, $^{1}J_{PC}$ = 97.4 Hz, i-Ph_2P of **2c-A**), 136.5 (dd, $^{1}J_{PC}$ = 97.3 Hz, $^{3}J_{PC}$ = 4.8 Hz, i-Ph_2P of **2c-D**), 132.8 (app t, $^{2}J_{PC}$ = 4.7 Hz, *o*-Ph_2P of **2c-D**), 132.7 (app t, $^{2}J_{PC}$ = 5.2 Hz, *o*-Ph_2P of **2c-A**), 130.5 (s, *p*-Ph_2P of **2c-D**), 130.0 (s, *p*-Ph_2P of **2c-A**), 127.9 (app t, $^{2}J_{PC}$ = 5.9 Hz, *m*-Ph_2P of both forms), 52.4 (br s, *C*$(CH_3)_3$ of **2c-A**), 52.0 (t, $^{2}J_{PC} \sim 2$ Hz, *C*$(CH_3)_3$ of **2c-D**), 38.2 (t, $^{1}J_{PC}$ = 63.1 Hz, PCH_2P of **2c-D**), 35.5 (t, $^{3}J_{PC}$ = 5.4 Hz, *C*$(CH_3)_3$ of **2c-D**), 33.8 (br s, *C*$(CH_3)_3$ of **2c-A**), 17.2

(t, $^1J_{PC}$ ~ 129 Hz, PCHP of **2c-A**). $^{31}P\{^1H\}$ NMR (202 MHz, CD_2Cl_2, 300 K): δ = 18.2 (**2c-A**, $\nu_{1/2}$ = 10 Hz), −11.9 (**2c-D**, $\nu_{1/2}$ = 14 Hz).

Preparation of Li compound 3a. Compound **2a** (1.00 g, 1.76 mmol) was suspended in THF (10 mL). A solution of *n*-BuLi (1.61 M in hexanes; 1.12 mL, 1.80 mmol) was prepared by dilution in THF (5 mL). Both vessels were cooled to −80 °C, and *n*-BuLi was added dropwise by cannulation onto **2a**. The resulting mixture was stirred at −80 °C for 15 min, and then the cold bath was removed. After a further 20 min, the solvent was evaporated and the vessel was taken into the glovebox. The residue was triturated with 10 mL pentane, the supernatant solution was discarded and the remaining solid was dried *in vacuo*, affording complex **3a** as a white powder in 94% yield (1.04 g). The purity of the material thus obtained (assessed by ^1H and ^{31}P NMR spectroscopy) was sufficient for further reaction. An analytically pure sample suitable for elemental analysis was obtained by recrystallization from a THF–*n*-pentane mixture.

Elemental analysis: calcd for $C_{41}H_{39}LiN_2OP_2$: C, 76.39; H, 6.10; N, 4.35. Found: C, 76.27; H, 6.00; N, 4.39. HRMS (ESI-neg): calcd for $C_{37}H_{31}N_2P_2$ $[M - Li - THF]^-$: 565.19570. Found: 565.19728 (0.9 ppm). ^1H NMR (500 MHz, CD_2Cl_2, 300 K): δ = 7.53 (m, 8H, *o*-Ph_2P), 7.24 (m, 4H, *p*-Ph_2P), 7.10 (m, 8H, *m*-Ph_2P), 6.88 (m, 4H, *m*-PhN), 6.53 (m, 6H, overlapping *o*- and *p*-PhN), 3.91 (m, 4H, OCH_2), 1.90 (m, 4H, CH_2), 1.28 (br s, 1H, PC*H*P). $^{13}C\{^1H\}$ NMR (126 MHz, CD_2Cl_2, 300 K): δ = 151.9 (s, i-PhN), 134.8 (d, $^1J_{PC}$ = 91.0 Hz, i-Ph_2P), 132.2 (app t, $^2J_{PC}$ = 4.6 Hz, *o*-Ph_2P), 130.2 (s, *p*-Ph_2P), 128.7 (s, *m*-PhN), 128.1 (app t, $^2J_{PC}$ = 5.4 Hz, *m*-Ph_2P), 122.7 (br s, *o*-PhN), 116.6 (s, *p*-PhN), 69.0 (s, OCH_2), 26.0 (s, CH_2), 19.0 (t, $^1J_{PC}$ = 137.5 Hz, PCHP). $^{31}P\{^1H\}$ NMR (202 MHz, CD_2Cl_2, 300 K): δ = 16.5 ($\nu_{1/2}$ = 184 Hz).

Preparation of Li compound 3b. Compound **2b** (0.93 g, 1.90 mmol) was suspended in THF (10 mL). A solution of *n*-BuLi (1.61 M in hexanes; 1.20 mL, 1.93 mmol) was prepared by dilution in THF (5 mL). Both vessels were cooled to −80 °C, and *n*-BuLi was added dropwise by cannulation onto **2b**. The resulting mixture was stirred at −80 °C for 15 min, and then the cold bath was removed. After a further 30 min, the solvent was evaporated and the vessel was taken into the glovebox. The residue was triturated with 10 mL pentane, the supernatant solution was discarded and the remaining solid was dried *in vacuo*, affording complex **3b** as a white powder in 75% yield (0.82 g). The purity of the material thus obtained (assessed by ^1H and ^{31}P NMR spectroscopy) was sufficient for further reaction. Single crystals suitable for X-ray diffraction were grown by slow diffusion of *n*-pentane into a THF solution of **3b** at −18 °C.

Elemental analysis: calcd for $C_{35}H_{43}LiN_2OP_2$: C, 72.90; H, 7.52; N, 4.86. Found: C, 71.57; H, 8.25; N, 4.85 (unsatisfactory, probably due to hydrolysis of the sample). HRMS (ESI-neg): calcd for $C_{31}H_{35}N_2P_2$ $[M - Li - THF]^-$: 497.22700. Found: 497.22810 (2.2 ppm). ^1H NMR (500 MHz, C_6D_6, 300 K): δ = 7.75 (m, 8H, *o*-Ph_2P), 7.10 (m, 12H, overlapping *m*- and *p*-Ph_2P), 3.76 (m, 4H, OCH_2), 3.47 (d of heptuplet, $^3J_{PH}$ = 21.7 Hz, $^3J_{HH}$ = 6.1 Hz, 2H, C*H*$(CH_3)_2$), 1.37 (m, 4H, CH_2), 1.33 (br s, 1H, PC*H*P), 1.26 (d, $^3J_{HH}$ = 6.1 Hz, 12H, CH(CH_3)$_2$). $^{13}C\{^1H\}$ NMR (126 MHz, C_6D_6, 300 K): δ = 140.5 (d, $^1J_{PC}$ = 85.0 Hz, i-Ph_2P), 132.2 (app t, $^2J_{PC}$ = 4.5 Hz, *o*-Ph_2P), 129.1 (s, *p*-Ph_2P), 127.2 (app t, $^2J_{PC}$ = 5.2 Hz, *m*-Ph_2P), 68.7 (s, OCH_2), 46.3 (t, $^2J_{PC}$ = 2.5 Hz, *C*H$(CH_3)_2$), 29.2 (t, $^3J_{PC}$ = 5.7 Hz, CH(*C*H_3)$_2$), 25.5 (s, CH_2), 17.9 (t, $^1J_{PC}$ = 141.6 Hz, P*C*HP). $^{31}P\{^1H\}$ NMR (202 MHz, C_6D_6, 300 K): δ = 21.4 ($\nu_{1/2}$ = 85 Hz).

Preparation of Li compound 3c. Compound **2c** (1.79 g, 3.30 mmol) was dissolved in THF (15 mL). A solution of *n*-BuLi (1.61 M in hexanes; 2.10 mL, 3.37 mmol) was prepared by dilution in THF (7 mL). Both vessels were cooled to −80 °C, and *n*-BuLi was added dropwise by cannulation onto **2c**. The resulting mixture was stirred at −80 °C for 15 min, and then the cold bath was removed. After a further 15 min, the solvent was evaporated, affording complex **3c** as a white powder in 76% yield (1.53 g). The purity of the material thus obtained (assessed by ^1H and ^{31}P NMR spectroscopy) was sufficient for further reaction. An analytically pure sample suitable for elemental analysis was obtained by recrystallization from a THF–*n*-pentane mixture. Single crystals suitable for X-ray diffraction were grown by slow diffusion of *n*-pentane into a THF solution of **3c** at −18 °C.

Elemental analysis: calcd for $C_{37}H_{47}LiN_2OP_2$: C, 73.49; H, 7.83; N, 4.63. Found: C, 73.31; H, 7.78; N, 4.71. HRMS (ESI-neg): calcd for $C_{33}H_{39}N_2P_2$ $[M - Li - THF]^-$: 525.25830. Found: 525.26019 (1.5 ppm). ^1H NMR (500 MHz, CD_2Cl_2, 300 K): δ = 7.62 (m, 8H, *o*-Ph_2P), 7.28 (m, 4H, *p*-Ph_2P), 7.20 (m, 8H, *m*-Ph_2P), 3.95 (m, 4H, OCH_2), 1.92 (m, 4H, CH_2), 1.09 (s, 18H, ^{t}Bu, *o*-Ph_2P), 0.47 (t, $^2J_{PH}$ = 4.9 Hz, 1H, PC*H*P). $^{13}C\{^1H\}$ NMR (126 MHz, CD_2Cl_2, 300 K): δ = 142.7 (d, $^1J_{PC}$ = 81.2 Hz, i-Ph_2P), 132.4 (app t, $^2J_{PC}$ = 4.9 Hz, *o*-Ph_2P), 128.9 (s, *p*-Ph_2P), 127.4 (app t, $^2J_{PC}$ = 5.1 Hz, *m*-Ph_2P), 68.8 (s, OCH_2), 51.4 (t, $^2J_{PC}$ = 3.9 Hz, *C*$(CH_3)_3$), 35.2 (t, $^3J_{PC}$ = 5.2 Hz, C(*C*H_3)$_3$), 26.0 (s, CH_2), 23.8 (t, $^1J_{PC}$ = 146.6 Hz, P*C*HP). $^{31}P\{^1H\}$ NMR (202 MHz, CD_2Cl_2, 300 K): δ = 10.4 ($\nu_{1/2}$ = 17 Hz).

Preparation of Ti complex 4a. Compound **3a** (1.00 g, 1.55 mmol) and Ti precursor (0.71 g, 1.55 mmol) were placed in a Schlenk vessel at −15 °C, and Et_2O (25 mL) was added by a syringe. The heterogeneous reaction mixture was stirred for 2 h, after which the cold bath was removed. The yellow suspension was stirred for another 20 min and filtered over Celite®. The insoluble solids deposited on the Celite® cake were rinsed with toluene, and the resulting yellow solution was evaporated. The crude product was taken into the glovebox and dissolved in THF (2 mL). The resulting solution was layered with *n*-pentane (25 mL) and stored at −18 °C for over two days. Complex **4a** was isolated as pale yellow crystals in 63% yield (0.45 g), which decomposes slowly (months) upon storage under N_2 at −18 °C. The material thus obtained contained 20 mol% of THF (assessed by ^1H NMR spectroscopy). Single crystals suitable for X-ray diffraction were obtained by slow diffusion of *n*-pentane into a CH_2Cl_2 solution of **4a** at −18 °C.

Elemental analysis: calcd for $C_{41}H_{39}ClN_3P_2Ti0.2{\cdot}THF$: C, 68.36; H, 5.71; N, 5.72. Found: C, 68.56; H, 5.47; N, 5.74. FTIR (ATR): 2958 (w), 1592 (m), 1485 (m), 1435 (m), 1264 (m),

1250 (m), 1236 (m), 1178 (m), 1108 (m), 974 (m), 965 (s), 819 (m), 798 (s), 740 (s), 715 (m), 694 (s), 506 (br, s), 229 (m) cm^{-1}. ^1H NMR (500 MHz, C_6D_6, 300 K): δ = 8.10 (m, 4H, *o*-Ph_2P), 7.69 (d, $^2J_{HH}$ = 8.4 Hz, 4H, *o*-PhN), 7.22 (m, 4H, *o*-Ph_2P), 7.08 (d, $^2J_{HH}$ = 7.8 Hz, 4H, *m*-PhN), 6.99 (m, 6H, overlapping *m*- and *p*-Ph_2P), 6.86 (t, $^2J_{HH}$ = 7.8 Hz, 2H, *p*-PhN), 6.72 (t, $^2J_{HH}$ = 7.4 Hz, 2H, *p*-Ph_2P), 6.55 (m, 4H, *m*-Ph_2P), 1.49 (br s, 1H, PC*H*P), 1.25 (s, 9H, TiN^{t}Bu). $^{13}C\{^1H\}$ NMR (126 MHz, C_6D_6, 300 K): δ = 151.1 (s, i-PhN), n.o. (i-Ph_2P), 132.9 (app t, $^2J_{PC}$ = 4.9 Hz, *o*-Ph_2P), 132.4 (app t, $^2J_{PC}$ = 5.4 Hz, *o*-Ph_2P), 132.2 (s, *p*-Ph_2P), 130.9 (s, *p*-Ph_2P), 128.9 (app t, $^2J_{PC}$ = 6.0 Hz, *m*-Ph_2P), 128.7 (s, *m*-PhN), 128.1 (app t, $^2J_{PC}$ = 6.1 Hz, *m*-Ph_2P hidden by solvent signal, visible only in DEPT spectra), 125.4 (app t, $^2J_{PC}$ = 4.7 Hz, *o*-PhN), 123.0 (br s, *p*-PhN), 70.3 (s, TiN*C*$(CH_3)_3$), 31.6 (s, TiNC(*C*$H_3)_3$), 7.87 (t, $^1J_{PC}$ = 122.2 Hz, P*C*HP). $^{31}P\{^1H\}$ NMR (202 MHz, C_6D_6, 300 K): δ = 22.2 ($\nu_{1/2}$ = 12 Hz).

Preparation of Ti complex 4b. Compound **3b** (0.500 g, 0.867 mmol) and Ti precursor (0.395 g, 0.867 mmol) were placed in a Schlenk vessel at −15 °C, and Et_2O (15 mL) was added by a syringe. The heterogeneous reaction mixture was stirred for 2 h, after which the cold bath was removed. The yellow suspension was stirred for another 30 min, filtered over Celite®, and the resulting yellow solution was evaporated. The crude product was taken into the glovebox and dissolved in THF (2 mL). The resulting solution was layered with *n*-pentane (25 mL) and stored at −18 °C for over two days. Complex **4b** was isolated as pale yellow crystals in 59% yield (0.33 g). Single crystals suitable for X-ray diffraction (albeit with a high resolution factor) were obtained by slow diffusion of *n*-pentane into a THF solution of **4b** at −18 °C.

Elemental analysis: calcd for $C_{35}H_{44}ClN_3P_2Ti$: C, 64.47; H, 6.80; N, 6.44. Found: C, 64.32; H, 6.92; N, 6.34. FTIR (ATR): 3065 (w), 2860 (w), 2958 (w), 1434 (m), 1233 (m), 1174 (m), 1129 (m), 1110 (s), 1074 (m), 1064 (m), 989 (m), 897 (m), 827 (m), 811 (s), 800 (m), 744 (m), 716 (m), 689 (s), 565 (m), 558 (m), 523 (br, s), 502 (s), 489 (m), 319 (m) cm^{-1}. ^1H NMR (500 MHz, CD_2Cl_2, 300 K): δ = 7.86 (m, 4H, *o*-Ph_2P), 7.52 (t, $^2J_{HH}$ = 7.1 Hz, 2H, *p*-Ph_2P), 7.43 (t, $^2J_{HH}$ = 7.1 Hz, 4H, *m*-Ph_2P), 7.20 (t, $^2J_{HH}$ = 7.1 Hz, 2H, *p*-Ph_2P), 7.14 (m, 4H, *o*-Ph_2P), 7.01 (t, $^2J_{HH}$ = 7.2 Hz, 4H, *m*-Ph_2P), 3.32 (m, 2H, C*H*$(CH_3)_2$), 1.77 (d, $^3J_{HH}$ = 7.2 Hz, 6H, CH(C$H_3)_2$), 1.49 (br s, 1H, PC*H*P), 1.25 (s, 9H, TiN^{t}Bu), 0.91 (d, $^3J_{HH}$ = 7.2 Hz, 6H, CH(C$H_3)_2$). $^{13}C\{^1H\}$ NMR (126 MHz, CD_2Cl_2, 300 K): δ = 133.0 (dd, $^1J_{PC}$ = 98.2 Hz, $^3J_{PC}$ = 1.7 Hz, i-Ph_2P), 132.1 (app t, $^2J_{PC}$ = 5.0 Hz, *o*-Ph_2P), 132.1 (s, *p*-Ph_2P), 132.0 (app t, $^2J_{PC}$ = 5.4 Hz, *o*-Ph_2P), 131.1 (s, *p*-Ph_2P), 129.1 (dd, $^1J_{PC}$ = 94.8 Hz, $^3J_{PC}$ = 7.2 Hz, i-Ph_2P partially hidden under *m*-Ph_2P), 128.7 (app t, $^2J_{PC}$ = 6.0 Hz, *m*-Ph_2P), 128.4 (app t, $^2J_{PC}$ = 6.1 Hz, *m*-Ph_2P), 68.7 (s, TiN*C*$(CH_3)_3$), 48.7 (s, *C*H$(CH_3)_2$), 32.8 (s, TiNC(*C*$H_3)_3$), 27.4 (s, CH(*C*$H_3)_2$), 27.2 (app t, $^3J_{PC}$ = 5.5 Hz, CH(*C*$H_3)_2$), 4.9 (t, $^1J_{PC}$ = 120.1 Hz, P*C*HP). $^{31}P\{^1H\}$ NMR (202 MHz, CD_2Cl_2, 300 K): δ = 26.4 ($\nu_{1/2}$ = 36 Hz).

Preparation of Ti complex 4c. Compound **3c** (1.07 g, 1.77 mmol) and Ti precursor (0.806 g, 1.77 mmol) were placed in a Schlenk vessel at −15 °C, and Et_2O (30 mL) was added by a syringe. The heterogeneous reaction mixture was stirred for 2 h, after which the cold bath was removed. The yellow suspension was stirred for another 20 min, filtered over Celite®, and the resulting yellow solution was evaporated. The crude product was taken into the glovebox and dissolved in THF (2 mL). The resulting solution was layered with pentane (25 mL) and stored at −18 °C overnight. Complex **4c** was isolated as pale yellow crystals in 44% yield (0.53 g). A mixture of conformers was observed in solution (**4c-ax** and **4c-eq**), with **4c-ax** representing 88% of the mixture at 300 K in CD_2Cl_2. Single crystals suitable for X-ray diffraction were obtained by slow diffusion of *n*-pentane into a CH_2Cl_2 solution of **4c** at −18 °C.

Elemental analysis: calcd for $C_{37}H_{48}ClN_3P_2Ti$: C, 65.35; H, 7.11; N, 6.18. Found: C, 65.29; H, 6.99; N, 6.28. FTIR (ATR): 2957 (w), 1440 (m), 1433 (m), 1359 (m), 1352 (m), 1226 (m), 1182 (m), 1107 (s), 1066 (m), 1026 (m), 1003 (m), 982 (m), 974 (m), 845 (m), 833 (m), 788 (m), 763 (m), 734 (s), 693 (s), 683 (m), 581 (m), 575 (m), 546 (s), 522 (s), 494 (s), 383 (br, s) cm^{-1}. ^1H NMR (500 MHz, CD_2Cl_2, 300 K): δ = 8.18 (m, 4H, Ph_2P of **4c-eq**), 8.11 (m, 4H, *o*-Ph_2P of **4c-ax**), 7.51 (m, Ph_2P of **4c-eq**), 7.47 (m, 2H, *p*-Ph_2P of **4c-ax** overlapping with Ph_2P of **4c-eq**), 7.40 (m, 4H, *m*-Ph_2P of **4c-ax**), 7.28–7.15 (m, 6H, *p*-Ph_2P and *o*-Ph_2P of **4c-ax** overlapping with Ph_2P of **4c-eq**), 7.05–6.97 (m, 4H, *m*-Ph_2P of **4c-ax** overlapping with Ph_2P of **4c-eq**), 2.49 (t, $^2J_{PH}$ = 3.8 Hz, PC*H*P of **4c-eq**), 1.44 (s, 18H, PN^{t}Bu of **4c-ax**), 1.30 (two overlapping s, 9H, TiN^{t}Bu of **4c-ax** and **4c-eq**), 1.24 (s, PN^{t}Bu of **4c-eq**), 1.02 (br s, 1H, PC*H*P of **4c-ax**). $^{13}C\{^1H\}$ NMR (126 MHz, CD_2Cl_2, 300 K): δ = 136.3 (d, $^1J_{PC}$ = 90.8 Hz, i-Ph_2P of **4c-eq**), 135.4 (d, $^1J_{PC}$ = 96.9 Hz, i–Ph_2P of **4c-ax**), 133.2 (app t, $^2J_{PC}$ = 5.2 Hz, *o*-Ph_2P of **4c-ax**), 132.9 (app t, $^2J_{PC}$ = 5.5 Hz, Ph_2P of **4c-eq**), 132.5 (app t, $^2J_{PC}$ = 5.5 Hz, *o*-Ph_2P of **4c-ax**), 132.2 (app t, $^2J_{PC}$ = 5.3 Hz, Ph_2P of **4c-eq**), 131.6 (s, *p*-Ph_2P of **4c-ax**), 131.3 (s, Ph_2P of **4c-eq**), 131.0 (s, *p*-Ph_2P of **4c-ax**), 129.4 (dd, $^1J_{PC}$ = 97.0 Hz, $^3J_{PC}$ = 7.8 Hz, i-Ph_2P of **4c-ax**), 128.5 (app t, $^2J_{PC}$ = 6.0 Hz, *m*-Ph_2P of **4c-ax** overlapping with Ph_2P of **4c-eq**), 128.2 (app t, $^2J_{PC}$ = 6.1 Hz, *m*-Ph_2P of **4c-ax** overlapping with Ph_2P of **4c-eq**), 69.8 (s, TiN*C*$(CH_3)_3$ of **4c-eq**), 69.2 (s, TiN*C*$(CH_3)_3$ of **4c-ax**), 55.9 (app t, $^2J_{PC}$ = 2.6 Hz, PN*C*$(CH_3)_3$ of **4c-ax**), 54.9 (app t, $^2J_{PC}$ = 2.6 Hz, PN*C*$(CH_3)_3$ of **4c-eq**), 34.7 (app t, $^2J_{PC}$ = 3.5 Hz, TiN*C*$(CH_3)_3$ of **4c-ax**), 33.8 (app t, $^2J_{PC}$ = 4.2 Hz, TiN*C*$(CH_3)_3$ of **4c-eq**), 32.7 (s, TiNC(*C*$H_3)_3$ of **4c-ax**), 32.6 (s, TiNC(*C*$H_3)_3$ of **4c-eq**), 10.6 (app s, P*C*HP of **4c-eq**) 8.8 (t, $^1J_{PC}$ = 120.3 Hz, P*C*HP of **4c-ax**). $^{31}P\{^1H\}$ NMR (202 MHz, CD_2Cl_2, 300 K): δ = 22.7 ($\nu_{1/2}$ = 5 Hz, **4c-ax**), 15.6 ($\nu_{1/2}$ = 4 Hz, **4c-eq**).

Reaction of BIP ligands with [Ti(N^{t}Bu)Cl$_2$(Py)$_3$]

Ligands **2** (0.05 mmol) and [Ti(N^{t}Bu)$Cl_2(Py)_3$]·0.3CH_2Cl_2 (0.05 mmol, 1 eq.) were dissolved in d_8-THF and the solution was transferred into a J. Young NMR tube. The reaction mixture was analyzed by ^1H and ^{31}P NMR spectroscopy. The NMR tube was returned into the glovebox, KHMDS (10.0 mg, 1 equiv.) was added, and the mixture was analyzed again.

Hydrolysis/alcoholysis of Ti complexes

Complexes **4** (0.05 mmol) were dissolved in THF (between 0 and 1.5 mL depending on the quantity of water to be added). The required amount (1–4 eq., 0.5–2.0 mL) of stock solution of

water or ^{i}PrOH in THF (0.1 M) was added to this solution. The final volume was 2.0 mL. The reaction mixture was stirred for 20 min, then evaporated, and analyzed by ^{1}H and ^{31}P NMR spectroscopy. The spectra of **5a** and **5b** were found identical to the literature data (Br^- salts).[10] Compound **5c** (18.0 mg, 64%) was isolated as a white powder from a total hydrolysis experiment (2 equiv. H_2O).

Analytical data for 5c. HRMS (ESI-pos): calcd for $C_{33}H_{41}N_2P_2$ $[M + H]^+$: 527.27395. Found: 527.27199 (−3.7 ppm). ^{1}H NMR (500 MHz, $CDCl_3$, 300 K): δ = 7.64 (m, 8H, *o*-Ph_2P), 7.43 (t, $^{3}J_{HH}$ = 7.4 Hz, 4H, *p*-Ph_2P), 7.30 (m, 8H, *m*-Ph_2P), 7.40 (br s, 2H, N*H*), 2.09 (br s, 1H, PC*H*P), 1.10 (s, 18H, ^{t}Bu). $^{13}C\{^{1}H\}$ NMR (126 MHz, $CDCl_3$, 300 K): δ = 132.8 (app t, $^{2}J_{PC}$ = 5.5 Hz, *o*-Ph_2P), 131.8 (s, *p*-Ph_2P), 130.5 (d, $^{1}J_{PC}$ = 112.8 Hz, i-Ph_2P), 128.5 (app t, $^{2}J_{PC}$ = 6.4 Hz, *m*-Ph_2P), 53.9 (s, *C*$(CH_3)_3$), 31.9 (s, C(*C*$H_3)_3$), 16.3 (t, $^{1}J_{PC}$ = 135.8 Hz, P*C*HP). $^{31}P\{^{1}H\}$ NMR (202 MHz, $CDCl_3$, 300 K): δ = 27.2 ($\nu_{1/2}$ = 6 Hz).

Reaction of Ti complexes with hydroamination substrates

Complexes **4** (0.05 mmol) were dissolved in C_6D_6 (1.5 mL), and aniline (0.5 mmol, 10 equiv.) and phenylacetylene (0.5 mmol, 10 equiv.) were added. The mixture was transferred into a J. Young NMR tube and its evolution was checked by ^{1}H and ^{31}P NMR spectroscopy.

Representative procedure for the catalytic hydroamination of alkynes

In the glovebox, aniline (46 μL, 0.5 mmol) and phenylacetylene (55 μL, 0.5 mmol) were added to 1 mL of **4a** in C_6D_6 (solution prepared freshly by dissolving 45.0 mg of **4a** into 2.5 mL of C_6D_6). The reaction mixture was placed in a pressure tube closed by a Teflon® coated silicon seal, and heated to 105 °C. Upon cooling, the mixture was transferred into the glovebox, the seal was removed and the mixture was analyzed by ^{1}H NMR spectroscopy. A stock solution of 1,3,5-trimethoxybenzene in C_6D_6 (0.0102 M) was used throughout to enable quantitative analysis of reaction mixtures by ^{1}H NMR spectroscopy. To this end, spectra were recorded at 300 K on a Bruker 300 Avance III spectrometer (30° pulse, 50 s relaxation time, 4 scans). Reactions were run in duplicate, and relevant NMR signals were compared to the original samples (starting materials) or to those reported in the literature (products).[75,76]

X-ray diffraction analysis

Intensity data were collected on a Bruker APEX II at 115 K. The structures were solved by direct methods (SHELXS)[77] and refined with a full-matrix least-squares method based on F^2 (SHELXL).[77] All non-hydrogen atoms were refined with anisotropic parameters. Hydrogen atoms were included in their cal-

Table 5 Crystal data and structure refinement for **3b**, **3c**, **4a** and **4c**

	3b	3c	4a	4c
Empirical formula	$C_{35}H_{43}LiN_2OP_2$	$C_{37}H_{47}LiN_2OP_2$	$C_{41}H_{40}ClN_3P_2Ti$	$C_{37}H_{48}ClN_3P_2Ti$
Formula weight	576.59	604.64	720.05	680.07
Temperature/K	115	115	115	115
Crystal system	Triclinic	Triclinic	Orthorhombic	Triclinic
Space group	$P\bar{1}$	$P\bar{1}$	$Pna2_1$	$P\bar{1}$
a/Å	11.1903(7)	10.7879(3)	20.8571(5)	10.6873(2)
b/Å	12.0750(8)	11.0506(3)	9.9387(2)	10.9883(3)
c/Å	13.1287(9)	15.9326(5)	17.6389(4)	18.1781(4)
α/°	90.298(2)	90.684(2)	90	86.4350(10)
β/°	105.468(2)	94.916(2)	90	86.0200(10)
γ/°	107.231(2)	113.273(2)	90	65.2670(10)
Volume/Å^3	1626.15(19)	1736.23(9)	3656.41(14)	1932.95(8)
Z	2	2	4	2
$\rho_{calc.}$/mg mm^{-3}	1.178	1.157	1.308	1.168
μ/mm^{-1}	0.163	0.155	0.428	0.401
F(000)	616.0	648.0	1504.0	720.0
Crystal size/mm^3	0.25 × 0.25 × 0.2	0.6 × 0.5 × 0.4	0.17 × 0.15 × 0.1	0.25 × 0.25 × 0.2
Radiation	MoKα	MoKα	MoKα	MoKα
2*Θ* range for data collection	5.78 to 61.63°	4.64 to 55.13°	4.54 to 54.96°	4.67 to 54.97°
Index ranges	$-15 \le h \le 16$	$-14 \le h \le 13$	$-26 \le h \le 27$	$-13 \le h \le 13$
	$-17 \le k \le 17$	$-14 \le k \le 13$	$-12 \le k \le 12$	$-14 \le k \le 14$
	$-18 \le l \le 18$	$-20 \le l \le 20$	$-22 \le l \le 22$	$-23 \le l \le 23$
Reflections collected	62 708	12 733	26 450	16 536
Independent reflections	9351	7798	8303	8795
	R_{int} = 0.0353	R_{int} = 0.0137	R_{int} = 0.0313	R_{int} = 0.0172
	R_{sigma} = 0.0315	R_{sigma} = 0.0231	R_{sigma} = 0.0314	R_{sigma} = 0.0261
Data/restraints/parameters	9351/0/373	7798/0/408	8303/1/434	8795/0/397
Goodness-of-fit on F^2	1.040	1.076	1.059	1.060
Final *R* indexes [$I \ge 2\sigma(I)$]	R_1 = 0.0505	R_1 = 0.0404	R_1 = 0.0317	R_1 = 0.0404
	wR_2 = 0.1188	wR_2 = 0.1023	wR_2 = 0.0658	wR_2 = 0.1132
Final *R* indexes [all data]	R_1 = 0.0775	R_1 = 0.0443	R_1 = 0.0356	R_1 = 0.0458
	wR_2 = 0.1397	wR_2 = 0.1063	wR_2 = 0.0686	wR_2 = 0.1172
Largest diff. peak/hole/e Å^{-3}	1.25/−0.68	0.47/−0.29	0.22/−0.25	0.34/−0.37
Flack parameter	—	—	−0.02(3)	—
CCDC	987356	987357	987358	987359

culated positions and refined with a riding model. In **3c**, two carbon atoms of the THF ligand were found disordered and refined in two positions with occupation factors of 0.60/0.40. In **4c**, residual electron densities were found close to an inversion center, no attempts to model a solvent molecule were successful and the SQUEEZE[78] procedure in PLATON[79] was used to remove this contribution to the electron density in the final stages of refinement (void of 247 Å^3 and electron count of 62). Crystallographic data are reported in Table 5.

Acknowledgements

We thank the Conseil Régional de Bourgogne (PARI IME SMT08 program), the Ministère de l'Enseignement Supérieur et de la Recherche, and the Centre National de la Recherche Scientifique (CNRS) for financial support. We thank Miss M.-J. Penouilh and Dr F. Chaux Picquet for mass spectrometry analyses.

Notes and references

1 R. G. Cavell, R. P. Kamalesh Babu and K. Aparna, *J. Organomet. Chem.*, 2001, **617–618**, 158.
2 N. D. Jones and R. G. Cavell, *J. Organomet. Chem.*, 2005, **690**, 5485.
3 P. W. Roesky, *Z. Anorg. Allg. Chem.*, 2006, **632**, 1918.
4 T. Cantat, N. Mezailles, A. Auffrant and P. Le Floch, *Dalton Trans.*, 2008, 1957.
5 T. K. Panda and P. W. Roesky, *Chem. Soc. Rev.*, 2009, **38**, 2782.
6 S. T. Liddle, D. P. Mills and A. J. Wooles, *Chem. Soc. Rev.*, 2011, **40**, 2164.
7 R. A. Collins, J. Unruangsri and P. Mountford, *Dalton Trans.*, 2013, **42**, 759.
8 R. S. Rojas, A. R. Cabrera, B. C. Peoples, K. Spannhoff, M. Valderrama, R. Frohlich, G. Kehr and G. Erker, *Dalton Trans.*, 2012, **41**, 1243.
9 N. Kocher, D. Leusser, A. Murso and D. Stalke, *Chem. – Eur. J.*, 2004, **10**, 3622.
10 M. Demange, L. Boubekeur, A. Auffrant, N. Mezailles, L. Ricard, X. Le Goff and P. Le Floch, *New J. Chem.*, 2006, **30**, 1745.
11 L. Orzechowski, G. Jansen and S. Harder, *J. Am. Chem. Soc.*, 2006, **128**, 14676.
12 I. El-Zoghbi, M. Kebdani, T. J. J. Whitehorne and F. Schaper, *Organometallics*, 2013, **32**, 6986.
13 I. El-Zoghbi, E. Verguet, P. Oguadinma and F. Schaper, *Inorg. Chem. Commun.*, 2010, **13**, 529.
14 C. Bibal, M. Pink, Y. D. Smurnyy, J. Tomaszewski and K. G. Caulton, *J. Am. Chem. Soc.*, 2004, **126**, 2312.
15 O. J. Cooper, A. J. Wooles, J. McMaster, W. Lewis, A. J. Blake and S. T. Liddle, *Angew. Chem., Int. Ed.*, 2010, **49**, 5570.
16 P. Wei and D. W. Stephan, *Organometallics*, 2002, **21**, 1308.
17 R. G. Cavell, R. P. Kamalesh Babu, A. Kasani and R. McDonald, *J. Am. Chem. Soc.*, 1999, **121**, 5805.
18 Only **Ia** and **IIa** were structurally characterized.
19 Bochmann reported related Ti and Zr complexes with a κ^2-C,N coordination mode, see: (*a*) M. J. Sarsfield, M. Thornton-Pett and M. Bochmann, *J. Chem. Soc., Dalton Trans.*, 1999, 3329; (*b*) M. J. Sarsfield, M. Said, M. Thornton-Pett, L. A. Gerrard and M. Bochmann, *J. Chem. Soc., Dalton Trans.*, 2001, 822; (*c*) M. Said, M. Thornton-Pett and M. Bochmann, *J. Chem. Soc., Dalton Trans.*, 2001, 2844.
20 R. P. Kamalesh Babu, R. McDonald and R. G. Cavell, *Organometallics*, 2000, **19**, 3462.
21 N. Hazari and P. Mountford, *Acc. Chem. Res.*, 2005, **38**, 839.
22 A. R. Fout, U. J. Kilgore and D. J. Mindiola, *Chem. – Eur. J.*, 2007, **13**, 9428.
23 A. E. Guiducci, A. R. Cowley, M. E. G. Skinner and P. Mountford, *J. Chem. Soc., Dalton Trans.*, 2001, 1392.
24 A. E. Guiducci, C. L. Boyd and P. Mountford, *Organometallics*, 2006, **25**, 1167.
25 A. E. Guiducci, C. L. Boyd, E. Clot and P. Mountford, *Dalton Trans.*, 2009, 5960.
26 J. S. Johnson and R. G. Bergman, *J. Am. Chem. Soc.*, 2001, **123**, 2923.
27 I. Bytschkov and S. Doye, *Eur. J. Org. Chem.*, 2003, 935.
28 R. Severin and S. Doye, *Chem. Soc. Rev.*, 2007, **36**, 1407.
29 T. E. Müller, K. C. Hultzsch, M. Yus, F. Foubelo and M. Tada, *Chem. Rev.*, 2008, **108**, 3795.
30 A. Massard, PhD thesis, Université de Bourgogne, 2011.
31 C. Klemps, A. Buchard, R. Houdard, A. Auffrant, N. Mezailles, X. F. Le Goff, L. Ricard, L. Saussine, L. Magna and P. Le Floch, *New J. Chem.*, 2009, **33**, 1748.
32 Despite the somewhat misleading character of the P═N double bond depiction considering theoretical evidence gathered so far (see ref. 9–11), we decided to keep this widely used formalism for the sake of homogeneity. Obviously, the downside is that the choice of the terms alternating dipolar and dipolar becomes less intuitive with respect to the way structures are drawn. However, we feel they reflect more accurately the nature of the bonding in BIP ligands.
33 Similar metallation reactions have been reported by others, see ref. 19*a–c* and: (*a*) G. Aharonian, K. Feghali, S. Gambarotta and G. P. A. Yap, *Organometallics*, 2001, **20**, 2616; (*b*) C. Bibal, M. Pink, Y. D. Smurnyy, J. Tomaszewski and K. G. Caulton, *J. Am. Chem. Soc.*, 2004, **126**, 2312.
34 See ESI, Fig. S1;† the quality of the X-ray diffraction data is insufficient for a detailed discussion of bond distances and angles.
35 A. Buchard, A. Auffrant, L. Ricard, X. F. Le Goff, R. H. Platel, C. K. Williams and P. Le Floch, *Dalton Trans.*, 2009, 10219.
36 A. Buchard, R. H. Platel, A. Auffrant, X. F. Le Goff, P. Le Floch and C. K. Williams, *Organometallics*, 2010, **29**, 2892.
37 M. T. Gamer, M. Rastätter and P. W. Roesky, *Z. Anorg. Allg. Chem.*, 2002, **628**, 2269.

38 M. T. Gamer, M. Rastätter, P. W. Roesky, A. Steffens and M. Glanz, *Chem. – Eur. J.*, 2005, **11**, 3165.
39 T. K. Panda, A. Zulys, M. T. Gamer and P. W. Roesky, *J. Organomet. Chem.*, 2005, **690**, 5078.
40 T. K. Panda, A. Zulys, M. T. Gamer and P. W. Roesky, *Organometallics*, 2005, **24**, 2197.
41 M. T. Gamer, P. W. Roesky, I. Palard, M. Le Hellaye and S. M. Guillaume, *Organometallics*, 2007, **26**, 651.
42 S. T. Liddle, D. P. Mills, B. M. Gardner, J. McMaster, C. Jones and W. D. Woodul, *Inorg. Chem.*, 2009, **48**, 3520.
43 A. J. Wooles, O. J. Cooper, J. McMaster, W. Lewis, A. J. Blake and S. T. Liddle, *Organometallics*, 2010, **29**, 2315.
44 D. P. Mills, F. Moro, J. McMaster, J. van Slageren, W. Lewis, A. J. Blake and S. T. Liddle, *Nat. Chem.*, 2011, **3**, 454.
45 R. P. Kamalesh Babu, K. Aparna, R. McDonald and R. G. Cavell, *Organometallics*, 2001, **20**, 1451.
46 M. T. Gamer and P. W. Roesky, *Z. Anorg. Allg. Chem.*, 2001, **627**, 877.
47 M. S. Hill, P. B. Hitchcock and S. M. A. Karagouni, *J. Organomet. Chem.*, 2004, **689**, 722.
48 A. J. Wooles, M. Gregson, O. J. Cooper, A. Middleton-Gear, D. P. Mills, W. Lewis, A. J. Blake and S. T. Liddle, *Organometallics*, 2011, **30**, 5314.
49 A. J. Wooles, M. Gregson, S. Robinson, O. J. Cooper, D. P. Mills, W. Lewis, A. J. Blake and S. T. Liddle, *Organometallics*, 2011, **30**, 5326.
50 B. Cordero, V. Gomez, A. E. Platero-Prats, M. Reves, J. Echeverria, E. Cremades, F. Barragan and S. Alvarez, *Dalton Trans.*, 2008, 2832.
51 A. J. Blake, P. E. Collier, S. C. Dunn, W.-S. Li, P. Mountford and O. V. Shishkin, *J. Chem. Soc., Dalton Trans.*, 1997, 1549.
52 Despite repeated efforts, crystals of **4b** obtained in various solvents could not give satisfactory X-ray diffraction data. Nevertheless, a low quality set of data was obtained, revealing the same geometry (axial Cl isomer) as **4a** and **4c**; see ESI Fig. S2.†
53 S. Alvarez, *Dalton Trans.*, 2013, **42**, 8617.
54 THF and *n*-pentane were present in the sample as a result of co-crystallization with **4c**.
55 Since NOESY studies were inconclusive, the absolute configurations of both isomers were ascribed on the basis of X-ray diffraction data and DFT calculations.
56 H. Nagashima, T. Sue, T. Oda, A. Kanemitsu, T. Matsumoto, Y. Motoyama and Y. Sunada, *Organometallics*, 2006, **25**, 1987.
57 VT NMR up to 333 K did not show any sign of another isomer.
58 An interesting method to assess the relative importance of crystal packing effects (although beyond the scope of this study) is to calculate compliance constants, see for example: F. Breher, J. Grunenberg, S. C. Lawrence, P. Mountford and H. Rüegger, *Angew. Chem., Int. Ed.*, 2004, **43**, 2521.
59 N. Kaltsoyannis and P. Mountford, *J. Chem. Soc., Dalton Trans.*, 1999, 781.
60 In addition, replacing the N^{t}Bu imido by a less bulky NMe group does not decrease the P–N–C angles in **4d-ax** compared to **4c-ax** (in fact it becomes slightly wider), but it does make the N–Ti–N angle about 4° smaller, consistent with the notion that steric repulsion is responsible for the opening of this angle.
61 M. Rastatter, A. Zulys and P. W. Roesky, *Chem. Commun.*, 2006, 874.
62 A. Zulys, T. K. Panda, M. T. Gamer and P. W. Roesky, *Chem. Commun.*, 2004, 2584.
63 M. Rastätter, A. Zulys and P. W. Roesky, *Chem. – Eur. J.*, 2007, **13**, 3606.
64 J. Jenter, P. W. Roesky, N. Ajellal, S. M. Guillaume, N. Susperregui and L. Maron, *Chem. – Eur. J.*, 2010, **16**, 4629.
65 S. M. Guillaume, P. Brignou, N. Susperregui, L. Maron, M. Kuzdrowska and P. W. Roesky, *Polym. Chem.*, 2011, **2**, 1728.
66 S. M. Guillaume, P. Brignou, N. Susperregui, L. Maron, M. Kuzdrowska, J. Kratsch and P. W. Roesky, *Polym. Chem.*, 2012, **3**, 429.
67 R. G. Cavell, K. Aparna, R. P. Kamalesh Babu and Q. Wang, *J. Mol. Catal. A: Chem.*, 2002, **189**, 137.
68 M. S. Hill and P. B. Hitchcock, *J. Chem. Soc., Dalton Trans.*, 2002, 4694.
69 B. F. Straub and R. G. Bergman, *Angew. Chem., Int. Ed.*, 2001, **40**, 4632.
70 F. Pohlki and S. Doye, *Angew. Chem., Int. Ed.*, 2001, **40**, 2305.
71 In particular the fate of the substrates would need to be more rigorously investigated considering the difference between conversion values and the sum of products yields.
72 *Jaguar, v. 5.5*, Schrodinger, LLC, Portland, Oregon, 2003.
73 P. Imhoff, R. V. Asselt, C. J. Elsevier, K. Vrieze, K. Goubitz, K. F. Van Malssen and C. H. Stam, *Phosphorus, Sulfur Silicon Relat. Elem.*, 1990, **47**, 401.
74 S. Al-Benna, M. J. Sarsfield, M. Thornton-Pett, D. L. Ormsby, P. J. Maddox, P. Bres and M. Bochmann, *J. Chem. Soc., Dalton Trans.*, 2000, 4247.
75 L. L. Anderson, J. Arnold and R. G. Bergman, *Org. Lett.*, 2004, **6**, 2519.
76 S. Greenberg and D. W. Stephan, *Polym. Chem.*, 2010, **1**, 1332.
77 G. M. Sheldrick, *Acta Crystallogr., Sect. A: Fundam. Crystallogr.*, 2008, **64**, 112–122.
78 P. v. d. Sluis and A. L. Spek, *Acta Crystallogr., Sect. A: Fundam. Crystallogr.*, 1990, **46**, 194–201.
79 A. L. Spek, *J. Appl. Crystallogr.*, 2003, **36**, 7–13.